Journal of Nuclear Medicine, published on March 23, 2017 as doi:10.2967/jnumed.116.183020

Evaluation of the effect of fingolimod treatment on microglial activation using serial PET imaging in multiple sclerosis

Running title: TSPO-PET in fingolimod-treated RRMS

Marcus Sucksdorff[1,2*], Eero Rissanen[1,2*], Jouni Tuisku[2], Salla Nuutinen[1], Teemu Paavilainen[2], Johanna Rokka[2], Juha Rinne[1,2] and Laura Airas[1,2]

[1]Division of Clinical Neurosciences, Turku University Hospital, Kiinamyllynkatu 4-8, 20521 Turku, Finland;

[2]Turku PET Centre, Clinical Neurology, University of Turku, Kiinamyllynkatu 4-8, 20521 Turku, Finland

*Both authors contributed equally to this work.

Corresponding author: Dr. Marcus Sucksdorff**,** Division of Clinical Neurosciences, Turku University Hospital, PO Box 52, 20521 Turku, Finland

Phone: +358505508476

Email: marcus.sucksdorff@tyks.fi

Word count: 4997

Financial support: Finnish Academy, Sigrid Juselius Foundation, The Finnish MS Foundation, The Finnish Medical Foundation, The State Research Funding, Novartis Pharma and European Union's Seventh Framework Programme (FP7/2007-2013) under grant agreement n°HEALTH-F2-2011-278850 (INMiND).

ABSTRACT

Traditionally, multiple sclerosis (MS) has been considered a white matter (WM) disease with focal inflammatory lesions. It is, however, becoming clear that significant pathology, such as microglial activation, also takes place outside the plaque areas, i.e. in areas of normal appearing white matter (NAWM) and gray matter (GM). Microglial activation can be detected *in vivo* using an 18 kDa translocator protein (TSPO) binding radioligands and positron emission tomography (PET). It is unknown whether fingolimod affects microglial activation in MS. The aim of this study was to investigate whether serial PET can be used to evaluate the effect of fingolimod treatment on microglial activation. **Methods:** Ten relapsing-remitting MS (RRMS) patients were studied using the TSPO radioligand ^{11}C-(*R*)-PK11195. Imaging was performed at baseline and after 8 and 24 weeks of fingolimod treatment. Eight healthy individuals were imaged for comparison. Microglial activation was evaluated as distribution volume ratio (DVR) of ^{11}C-(*R*)-PK11195. **Results:** The patients had had MS for an average of 7.9 years (± 4.3, mean ± standard deviation (SD)), their total relapses averaged 4 ± 2.4, and their Expanded Disability Status Scale was 2.7 ± 0.5. The patients were switched to fingolimod due to safety reasons or therapy escalation. The mean washout period before the initiation of fingolimod was 2.3 ± 1.1 months. The patients were clinically stable on fingolimod. At baseline, microglial activation was significantly higher in the combined NAWM and GM areas of MS patients compared with healthy controls *(P* = 0.021). ^{11}C-(*R*)-PK11195 binding was reduced (−12.31%) within the combined T2 lesion area after six months of fingolimod treatment (*P* = 0.040), but not in the areas of NAWM or GM. **Conclusion:** Fingolimod treatment reduced microglial/macrophage activation at the site of focal inflammatory lesions, presumably by

preventing leukocyte trafficking from the periphery. It did not affect the widespread, diffuse microglial activation in the NAWM and GM. The study opens new vistas for designing future therapeutic studies in MS that use the evaluation of microglial activation as an imaging outcome measure.

Key words: Multiple sclerosis, PET imaging, TSPO, fingolimod, microglia

INTRODUCTION

In MS, neuroinflammation and neurodegeneration are two main components in the disease pathogenesis. Usually, the disease initiates as RRMS, where focal demyelination of the cerebral WM is the hallmark of the disease. At an average of 10 years after disease onset, RRMS shifts into secondary progressive MS and slowly leads to disability (*1*). Thus far, prevention of worsening of progressive MS has proven a major challenge, whereas great advances have been achieved in developing treatments for RRMS (*2*). This likely reflects the differences in the pathogenic mechanisms behind the respective disease subtypes. In RRMS, the major determinant driving the onset of relapses and the focal inflammatory lesions in the central nervous system (CNS) is the over-reactivity of the adaptive immune system, with resulting inflammatory cell trafficking from the periphery into the CNS (*1*). Patients with progressive disease, instead, present with chronic lesions with or without microglial activation (i.e. chronic active or chronic inactive lesions), and widespread microglial activation in the NAWM, which colocalizes with signs of neuronal damage (*3,4*). The microglial activation can be detected *in vivo* using PET and radioligands binding to an 18 kDa translocator protein (TSPO), which is expressed by activated microglial cells (*5-7*). It has however become clear that "activated" microglia consist of a wide array of microglial phenotypes, some of which are likely beneficial and contribute to clearing of debris, whereas some are pro-inflammatory and contribute to the relentless CNS damage related to progressive MS (*8,9*). Presently, these different phenotypes cannot be distinguished *in vivo*.

Fingolimod is the first oral disease-modifying therapy (DMT) developed for the treatment of RRMS. It blocks the egress of lymphocytes from secondary lymphoid tissues, and thereby prevents their entry into the CNS (*10,11*). In addition, being strongly lipophilic, fingolimod penetrates into the CNS and binds to sphingosine 1 phosphate receptor on CNS-resident glial and neural cells (*12*). Importantly, in animal models of MS, fingolimod modulates microglial and astroglial cells (*13-15*), which can be detected *in vivo* as a diminished TSPO ligand signal (*13*). Hence, fingolimod also has the potential to directly alleviate inflammation and neurodegeneration contained within the CNS of MS patients. However, in a recent study of primary progressive MS, fingolimod was proven ineffective in halting the disease progression (*16*).

Given the suspected role of activated microglial cells in MS, TSPO-PET in the NAWM has been suggested to be a potential surrogate outcome measure in trials of progressive MS (*5-7*). Thus far, the effect of any DMT on microglial activation has been evaluated in only one MS study (*17*). The aim of the present study was to determine the kinetics of microglial activation in various brain areas of a cohort of RRMS patients before and after fingolimod treatment using serial *in vivo* TSPO imaging. Furthermore, we wanted to evaluate whether in this cohort of RRMS patients with a disease duration averaging eight years, signs of microglial activation could already be seen outside the focal lesions.

MATERIALS AND METHODS

Study Subjects

The study was performed as an academic, investigator-initiated study at Turku PET

Centre and Turku University Hospital. The study protocol was approved by the Ethics Committee of the Hospital District of Southwest Finland. The study was registered to ClinicalTrials.gov (identifier NCT02139696). All participants signed a written informed consent according to the Declaration of Helsinki.

Patients with RRMS diagnosed according to the 2005 revised McDonald criteria (*18*), who were initiating treatment with oral 0.5 mg fingolimod daily were recruited from a single center. Key eligibility criteria were age 18–65 years, and an RRMS diagnosis for more than 5 years prior to enrolment and a neurologist's treatment decision of switching from previous treatment to fingolimod according to label. Disease duration was calculated as the time from the first demyelinating event to the first PET scan. A minimum washout period of 1 month after previous DMT was required.

Exclusion criteria included corticosteroid treatment within 30 days of evaluation, active neurological or autoimmune disease other than MS, or another comorbidity considered significant, inability to tolerate PET or magnetic resonance imaging (MRI) and a current or desired pregnancy in the 6 months following study enrolment.

Procedures

One of eleven recruited patients withdrew from the study after baseline imaging. 10 patients were imaged both at baseline and after 24 weeks of fingolimod treatment. They were on average 42 years old (SD 9.0). Seven patients underwent PET and MRI also after 6−8 weeks (range 53−102 days). Expanded Disability Status Scale, safety evaluation and recording of relapses were performed at baseline, after 6−8 weeks and 24 weeks of

fingolimod treatment (Fig. 1). The baseline PET were compared with historical PET data (with identical imaging methodology) from eight healthy individuals (six women, two men, mean age 49.8 years (SD 7.9, range 42–61 years)).

Outcomes

The primary outcome was the change in microglial activation after 24 weeks of fingolimod treatment. In addition, TSPO binding was evaluated after 6−8 weeks of treatment ($n = 7$). We also evaluated the effect of fingolimod treatment on MRI parameters. Finally, we evaluated how microglial activation at baseline correlated with MS duration, age and washout period before initiation of fingolimod treatment. We also evaluated how microglial activation correlated to duration of treatment.

MRI and Data Analysis

For the evaluation of MS pathology and for the acquisition of anatomical reference for the PET images, conventional MRI was performed with 3 tesla Philips Ingenuity TF PET/magnetic resonance scanner. MRI of the control group was performed with Philips Gyroscan Intera 1.5 tesla Nova Dual scanner (Philips, Best, the Netherlands). The routine sequences included axial T2, 3D fluid-attenuated inversion recovery, 3DT1 and 3DT1 with gadolinium enhancement.

For each patient, the T1 image at the first time point was co-registered in statistical parametric mapping (SPM8, version 8; Wellcome Trust Centre for Neuroimaging) to the sum image of realigned PET frames of the first session. All the other magnetic resonance

images were then co-registered to the T1 image of the first session. For each time point, the MS lesions were identified using the Lesion Segmentation Tool (a toolbox running in SPM8) (*19*) as described previously (*6*). The resulting lesion masks were used to fill the corresponding T1 image with the lesion filling tool in Lesion Segmentation Tool. The filled T1 was then used for segmenting GM and WM volumes with Freesurfer 5.3 software (http://surfer.nmr.mgh.harvard.edu/).

The volumes of T2 lesion masks acquired with Lesion Segmentation Tool were used for the T2 lesion load evaluation. Additionally, for each patient the Lesion Segmentation Tool masks at each time point were combined to a unified lesion region of interest (ROI). An average filled T1 image was also calculated from the filled T1 images of all MRI sessions and it was used for ROI delineation for cerebellum, striatum, thalamus, WM and cortical GM with Freesurfer. Finally, NAWM ROI was created by removing the lesion ROI from the WM ROI. The mixed GM and WM region contains the cortical GM, subcortical GM structures and the WM (NAWM and WM lesions), thus representing the global brain parenchyma.

^{11}C-(*R*)-PK11195 Radioligand Production and PET

The radiochemical synthesis of ^{11}C-(*R*)-PK11195 was performed as described before (*6*). The injected doses in each evaluated group did not differ from each other (data not shown). PET was performed with a brain-dedicated ECAT High-Resolution Research Tomograph scanner (CTI/Siemens) with an intrinsic spatial resolution of approximately 2.5 millimeter (*20*). First, a 6-minute transmission scan for attenuation correction was

obtained using a ^{137}Cs point source. Thereafter, 60-minute dynamic imaging was started simultaneously with the intravenous, bolus injection of the radioligand. Head movements were minimized using a thermoplastic mask.

PET Analysis

Image reconstruction was performed using 17 time frames as described previously (*6*). The dynamic data were then smoothed using a Gaussian 2.5-millimeter post-reconstruction filter (*6*). Possible displacements between frames were corrected using mutual information realignment in SPM8. For each patient, the PET images from the subsequent sessions were co-registered to the PET image of the first session using the sum images of each session. Finally, all images were resliced to match magnetic resonance voxel size of 1 millimeter.

For the estimation of ^{11}C-(*R*)-PK11195 DVR, the time–activity curve corresponding to a reference region devoid of specific TSPO binding was acquired for each PET session using a supervised cluster algorithm with 4 predefined kinetic tissue classes (SuperPK software) as described previously (*6*). As an additional step, the intersection of the clustered reference region maps within each subject's PET sessions was calculated and this region was then used to extract the individual reference region for each PET session. The reference tissue input Logan method, with a 20−60-minute time interval, was applied to the regional time activity curves using the supervised cluster algorithm gray reference input.

In order to correct for the partial volume effect caused by differences in ^{11}C-(*R*)-PK11195 binding between adjacent ROIs and by increased radioligand binding in the meningeal, vascular, bone and soft tissue next to cortical GM, a partial volume correction using the Geometric Transfer Matrix method (*21*) was performed for all regional time activity curves. Gaussian function with 2.5 millimeter full width at half maximum was used to approximate the scanner point spread function, and for each cortical region a corresponding background ROI was used to correct for the background activity.

Statistical Analyses

The statistical analyses were performed using SPSS (version 23, IBM Statistics). The data distribution was evaluated with Shapiro-Wilk test. When normally distributed, the group characteristics were reported as mean and SD. Non-normally distributed variables were reported as medians and interquartile range. The comparisons of the imaging parameters between healthy controls and RRMS patients were performed using analysis of covariance with age as a covariate due to the different, but overlapping distributions of age. In order to rule out the possible effect of volumetric changes in the DVR estimates, correlational analyses between the changes in T2 lesional, NAWM, cortical GM and total cerebral volumes and the changes in respective DVRs in these ROIs were examined using Spearman correlation.

The analysis of the serial PET data was carried out with repeated measures analysis of variance with Bonferroni correction. Other pairwise comparisons were performed with non-parametric Mann-Whitney U-test or Related Samples Wilcoxon Signed Rank Test,

wherein the non-parametric tests were chosen due to the low number of subjects per group. The associations between variables were analyzed with Spearman correlation. *P* value < 0.05 was considered statistically significant for all analyses unless stated otherwise.

Based on earlier ^{11}C-(*R*)-PK11195 studies (*6,17*), we estimated that a sample size of 10 subjects per group would suffice to reveal a 15% change between groups and a 5% change between the time points in the ^{11}C-(*R*)-PK11195 DVR within one examined ROI. However, due to the pilot nature of this study, a detailed á priori sample size calculation for repeated measures analysis of variance was unfeasible due to lack of detailed data on the expected effect size and variance with a function of time.

RESULTS

Clinical Characteristics of the Subjects

All participants were relapse-free for at least 3 months before the initial PET scan (median 9.6 months, range 3−77 months). The mean disease duration was 7.9 years (SD 4.3) and total relapse number averaged four (SD 2.4). The patients were switched to fingolimod because of safety reasons or therapy escalation. The mean washout period before the initiation of fingolimod treatment was 2.3 (SD 1.1) months. All patients were clinically and radiologically (MRI) stable during the entire study, there were no gadolinium-enhancing lesions, and no adverse events occurred (Supplemental Tables 1−2). The subject demographics are shown in Supplemental Table 3.

^{11}C-(*R*)-PK11195 Binding at the Beginning of Fingolimod Treatment

Microglial activation measured as ^{11}C-(*R*)-PK11195 DVR was significantly higher among the MS patients (n = 10) compared to healthy controls in the combined NAWM and GM area (P = 0.021) at baseline. Similarly, ^{11}C-(*R*)-PK11195 binding in thalami was stronger among MS patients than in controls (P = 0.006). In the separate NAWM, and cortical GM ROIs, there was a non-significant trend towards higher ^{11}C-(*R*)-PK11195 DVR in MS patients compared to controls (P = 0.096 and P = 0.052, respectively). In other ROIs, no significant differences were found between the groups (Fig. 2A; Supplemental Table 1).

^{11}C-(*R*)-PK11195 Binding Was Reduced in T2 Lesions after Six Months of Fingolimod Treatment Compared to Baseline

Ten participants underwent PET and MRI at baseline before initiating fingolimod treatment and again after 6 months. Fingolimod treatment was initiated within a week of baseline imaging, and the mean time between the PET scans was 190 days (range 141−267 days, Fig. 1). ^{11}C-(*R*)-PK11195 binding was reduced in the combined T2 lesion area after six months of treatment with fingolimod (−12.31%; P = 0.040) but not in other brain areas (Fig. 2B; Supplemental Table 1).

Serial ^{11}C-(*R*)-PK11195 Imaging during Fingolimod Treatment

Seven participants were scanned three times; first at baseline and again 2 and 6 months following the treatment initiation (Fig. 1). When three serial DVRs were evaluated, no statistically significant alterations were observed in any of the ROIs at group level (Fig. 2C; Supplemental Table 2). Interestingly, there was a slight increase in ^{11}C-(*R*)-PK11195

DVR in five out of seven patients in the NAWM and in six out of seven patients in cortical GM during the first two months of fingolimod treatment (Fig. 3).

Longer Washout Period, Longer Disease Duration and Higher Age Associate with Higher Microglial Activation in the NAWM

Treatment-free periods before fingolimod initiation varied between 30−131 days and interestingly, there was a non-significant trend for a correlation between longer washout period and higher NAWM DVR at baseline (n = 10, Spearman correlation 0.616, P = 0.058; Fig. 4A). Moreover, a higher baseline DVR in the NAWM was associated with longer disease duration (Spearman correlation 0.754, P = 0.012, Fig. 4B). There was a slight trend between longer fingolimod treatment and lower DVR in the NAWM in the 2nd and 3rd imaging time points, but this was statistically non-significant (Spearman correlation 0.238, P = 0.358, Fig. 4C). Furthermore, higher age correlated with higher DVR in the NAWM among MS patients (Spearman correlation 0.636, P = 0.048, Fig. 4D).

Power and Sample Size Analyses for Future Studies

Using the findings of the present study we wanted to calculate the sample size needed to demonstrate a statistically significant alteration in microglial activation within the NAWM. We discovered that in order to reveal a ±5% treatment effect with a statistical significance of $P < 0.05$, the sample size and the respective statistical power for a 5% increase between baseline and two months is n = 13 (power 0.907). For a 5% decrease both in 2 to 6 month, and 2 month to 1 year intervals the sample size is n = 14 (power 0.913).

DISCUSSION

This study used ^{11}C-(*R*)-PK11195 binding to measure the degree of microglial activation in MS patients before and after fingolimod treatment. Microglial activation was reduced after six months of fingolimod treatment in areas corresponding to focal T2 lesions. Microglial activation in the NAWM or GM was not affected. Microglial activation correlates with neurodegenerative changes related to MS progression (*3*,*22*) and it is conceivable that modulation of microglial activation might actually alleviate degeneration and decelerate the disease progression. The effects of DMTs on microglial activation in the NAWM in MS have thus far remained unclear. In the one previously published study, where MS treatment effect on microglial activation was evaluated, ^{11}C-(*R*)-PK11195 imaging was performed before and after one year of treatment with glatiramer acetate (*17*). In the present study we opted to image at earlier time points to understand the kinetics of treatment-associated alterations in microglial activation. We used the ^{11}C-(*R*)-PK11195 radioligand despite of its shortcomings, such as the limited signal-to-noise ratio. It is a widely and successfully used TSPO binding radioligand in the study of neurodegenerative disease and particularly, the advanced and reliable quantification methods available for this ligand make it useful for clinical assessment of brain pathology (*23*).

We compared the degree of microglial activation among MS patients at the beginning of fingolimod treatment to a control group of healthy individuals, and in this evaluation, the DVR in the combined NAWM and GM area was higher in the patient group than in the control group. The control group was somewhat older than the patient group, and it is possible that this slightly affected the results of the comparison of the DVRs in

individual ROIs in MS vs. controls, despite the attempt to statistically control for this by performing the comparison between MS patient and control DVRs using analysis of covariance with age as a covariate. In individual evaluation of NAWM and cortical GM ROIs, there was a strong, although non-significant, trend towards higher ^{11}C-(*R*)-PK11195 DVR in MS patients ($P = 0.096$ and $P = 0.052$, respectively) suggesting that the disease-related pathology had already started to spread outside the focal lesions and manifested as diffuse microglial activation. Moreover, the baseline DVR tended to correlate with the duration of the washout period, which might be relevant to the returning inflammatory activity after a DMT cessation; the longer the washout period, the higher the microglial activation at baseline among MS patients.

Based on our results, it seems evident that in the short term, the positive fingolimod treatment effect in MS comes from the prevention of focal inflammatory activity. This result is in line with larger studies using MRI as an outcome measure, which demonstrate a reduction in focal inflammatory activity after fingolimod treatment (*24*). Our results suggest that there are perhaps no direct effects mediated by fingolimod binding to sphingosine 1 phosphate receptors on microglial cells. Rather, after 2 months of treatment, ^{11}C-(*R*)-PK11195 binding increased slightly in five out of seven patients in the NAWM and in six out of seven patients in cortical GM. This might be a reflection of the still increasing inflammatory activity emerging from the peripheral immune system after the previous DMT cessation. In line with this, our patients also demonstrated a slight increase in T2 lesion load in the respective time point.

A small number of study subjects is a clear limitation of our study. Being the first study to incorporate serial TSPO-PET within a relatively short time frame in MS, the estimation of an appropriate sample size versus statistical power was challenging. The small number of subjects was probably the reason why we found no statistically significant alterations in several of the measured parameters. The reproducibility of ^{11}C-(*R*)-PK11195 imaging using an older generation HR+ scanner and the supervised clustering algorithm has proven feasible among healthy controls (*25*), but no data have yet existed on the repeatability of ^{11}C-(*R*)-PK11195 PET imaging in MS using higher resolution PET scanners, such as HRRT. This has to be taken into consideration when interpreting the results on radioligand binding especially in the non-lesional areas with lower variance. Our results also show that the washout period needs to be taken into account when designing TSPO-PET studies. To catch the pivot point of the highest TSPO binding after a drug-free washout period, we recommend obtaining the first PET image 2−3 months after the initiation of DMT (Fig. 5). If comparisons are to be done to a baseline image obtained immediately before the initiation of treatment, a longer follow-up should be considered. Our estimates show that with such a design one should be able to reach adequate statistical power with a feasible number of study subjects in terms of radiation safety and imaging costs. Based on the power calculations and the results of the present study, 15 patients per study group should be enough to reach sufficient statistical power to demonstrate the effect of fingolimod on microglial activation within the NAWM. The magnitude of the possible treatment effect of other DMTs on TSPO binding cannot, however, be predicted only from these results. Thus, there remains a challenge with power calculations for the future TSPO-PET treatment studies with other DMTs in MS. Taking into account the lessons learned from the present

study, we suggest a putative design for performing short-term studies evaluating the treatment effects of DMTs on diffuse microglial activation in MS (Fig. 5). Here, the recommended number of study subjects can be applied with confidence only to fingolimod studies. Finally, TSPO imaging has limitations in terms of identifying a particular microglial phenotype, and efforts are continuing for development of better PET ligands to differentiate between microglial cells with different functions.

CONCLUSION

In conclusion, the present study is the first one to apply serial TSPO-PET to evaluate microglial response to a DMT in MS. A reduction in microglial/macrophage activation was demonstrated after six months of fingolimod treatment in brain areas corresponding to T2 lesions, but no alteration in radioligand binding was observed in the NAWM or GM. The study demonstrates the possibilities and challenges of TSPO-PET in longitudinal evaluation of microglial activation status in response to treatment and opens new vistas for designing future therapeutic studies that use the evaluation of microglial activation as an imaging outcome measure.

ACKNOWLEDGEMENTS

We are thankful to all subjects participating in the study and making it possible.

REFERENCES

1. Compston A, Coles A. Multiple sclerosis. *Lancet.* 2008;372:1502-1517.

2. Ontaneda D, Fox RJ, Chataway J. Clinical trials in progressive multiple sclerosis: lessons learned and future perspectives. *Lancet Neurol.* 2015;14:208-223.

3. Frischer JM, Bramow S, Dal-Bianco A, et al. The relation between inflammation and neurodegeneration in multiple sclerosis brains. *Brain.* 2009;132:1175-1189.

4. Mahad DH, Trapp BD, Lassmann H. Pathological mechanisms in progressive multiple sclerosis. *Lancet Neurol.* 2015;14:183-193.

5. Banati RB, Newcombe J, Gunn RN, et al. The peripheral benzodiazepine binding site in the brain in multiple sclerosis: quantitative in vivo imaging of microglia as a measure of disease activity. *Brain.* 2000;123:2321-2337.

6. Rissanen E, Tuisku J, Rokka J, et al. In vivo detection of diffuse inflammation in secondary progressive multiple sclerosis using positron emission tomography imaging and radioligand [11C]PK11195. *J Nucl Med.* 2014;55:939-944.

7. Politis M, Giannetti P, Su P, et al. Increased PK11195 PET binding in the cortex of patients with MS correlates with disability. *Neurology.* 2012;79:523-530.

8. Howell OW, Rundle JL, Garg A, Komada M, Brophy PJ, Reynolds R. Activated microglia mediate axoglial disruption that contributes to axonal injury in multiple sclerosis. *J Neuropathol Exp Neurol.* 2010;69:1017-1033.

9. Boche D, Perry VH, Nicoll JA. Review: activation patterns of microglia and their identification in the human brain. *Neuropathol Appl Neurobiol.* 2013;39:3-18.

10. Matloubian M, Lo CG, Cinamon G, et al. Lymphocyte egress from thymus and peripheral lymphoid organs is dependent on S1P receptor 1. *Nature.* 2004;427:355-360.

11. Mandala S, Hajdu R, Bergstrom J, et al. Alteration of lymphocyte trafficking by sphingosine-1-phosphate receptor agonists. *Science.* 2002;296:346-349.

12. Soliven B, Miron V, Chun J. The neurobiology of sphingosine 1-phosphate signaling and sphingosine 1-phosphate receptor modulators. *Neurology.* 2011;76:S9-14.

13. Airas L, Dickens A, Elo P, et al. In vivo positron emission tomography imaging demonstrates diminished microglial activation after fingolimod treatment in an animal model of multiple sclerosis. *J Nucl Med.* 2015;56:305-310.

14. Colombo E, Di Dario M, Capitolo E, et al. Fingolimod may support neuroprotection via blockade of astrocyte nitric oxide. *Ann Neurol.* 2014;76:325-337.

15. Choi JW, Gardell SE, Herr DR, et al. FTY720 (fingolimod) efficacy in an animal model of multiple sclerosis requires astrocyte sphingosine 1-phosphate receptor 1 (S1P1) modulation. *Proc Natl Acad Sci U S A.* 2011;108:751-756.

16. Lublin F, Miller DH, Freedman MS, et al. Oral fingolimod in primary progressive multiple sclerosis (INFORMS): a phase 3, randomised, double-blind, placebo-controlled trial. *Lancet.* 2016;387:1075-1084.

17. Ratchford JN, Endres CJ, Hammoud DA, et al. Decreased microglial activation in MS patients treated with glatiramer acetate. *J Neurol.* 2012;259:1199-1205.

18. Polman CH, Reingold SC, Banwell B, et al. Diagnostic criteria for multiple sclerosis: 2010 revisions to the McDonald criteria. *Ann Neurol.* 2011;69:292-302.

19. Schmidt P, Gaser C, Arsic M, et al. An automated tool for detection of FLAIR-hyperintense white-matter lesions in multiple sclerosis. *Neuroimage.* 2012;59:3774-3783.

20. de Jong HW, van Velden FH, Kloet RW, Buijs FL, Boellaard R, Lammertsma AA. Performance evaluation of the ECAT HRRT: an LSO-LYSO double layer high resolution, high sensitivity scanner. *Phys Med Biol.* 2007;52:1505-1526.

21. Rousset OG, Ma Y, Evans AC. Correction for partial volume effects in PET: principle and validation. *J Nucl Med.* 1998;39:904-911.

22. Moll NM, Rietsch AM, Thomas S, et al. Multiple sclerosis normal-appearing white matter: pathology-imaging correlations. *Ann Neurol.* 2011;70:764-773.

23. Airas L, Rissanen E, Rinne J. Imaging neuroinflammation in multiple sclerosis using TSPO PET. *Clin Transl Imaging.* 2015;3:461-473.

24. Kappos L, Antel J, Comi G, et al. Oral fingolimod (FTY720) for relapsing multiple sclerosis. *N Engl J Med.* 2006;355:1124-1140.

25. Turkheimer FE, Edison P, Pavese N, et al. Reference and target region modeling of [11C]-(R)-PK11195 brain studies. *J Nucl Med.* 2007;48:158-167.

FIGURES

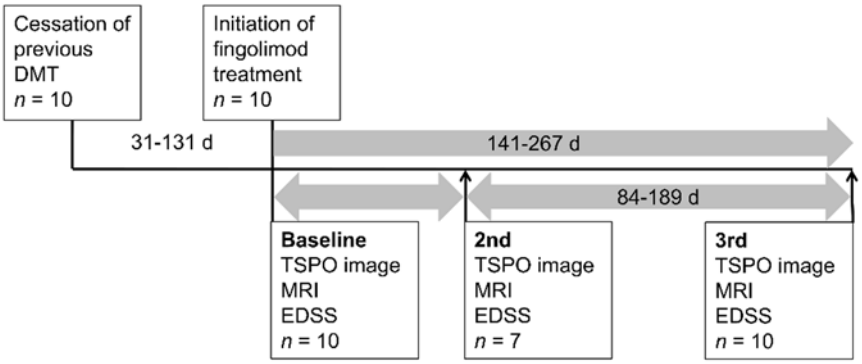

FIGURE 1. Schematic representation of the study timeline.

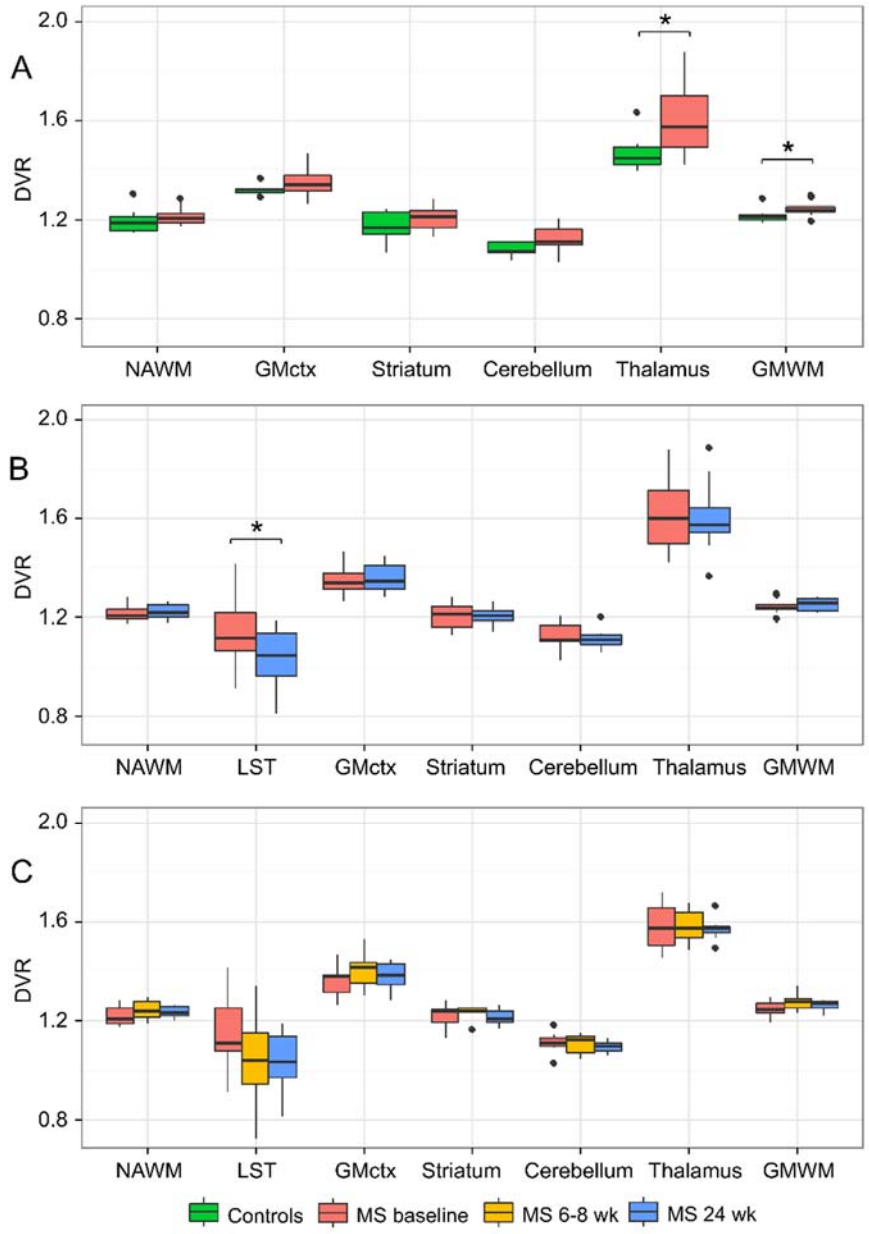

FIGURE 2. Region of interest-specific ^{11}C-(*R*)-PK11195 DVR values by group and imaging time point. The results are visualized as boxplots showing median DVR values with first and third quartiles. (A) Healthy controls (*n* = 8) and RRMS patients (*n* = 10) at baseline. (B) RRMS patients (*n* = 10) at baseline and at six-month time points and (C) RRMS patients (*n* = 7) at baseline, 2 months and 6 months.

* Statistically significant group difference at the level of $P < 0.05$ in analysis of covariance with age as covariate. Whiskers are calculated using formula 1.5 * interquartile range. Data beyond the end of the whiskers are outliers and plotted as points.

DVR = distribution volume ratio; GMctx = cortical gray matter; NAWM = normal appearing white matter; RRMS = relapsing-remitting multiple sclerosis; LST = area representing the lesion mask, which contains all T2 lesion areas in the corresponding magnetic resonance imaging; GMWM = combined gray matter and white matter areas

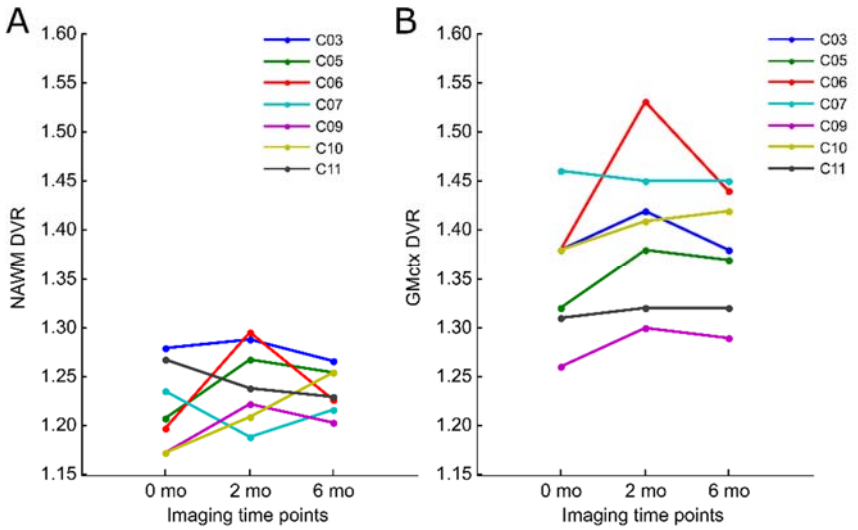

FIGURE 3. Serial positron emission tomography imaging results. Individual ^{11}C-(*R*)-PK11195 DVR values are shown in (A) NAWM and (B) normal appearing cortical gray matter at baseline, 2-month and 6-month time points in seven RRMS patients with longitudinal positron emission tomography data.

DVR = distribution volume ratio; NAWM = normal appearing white matter

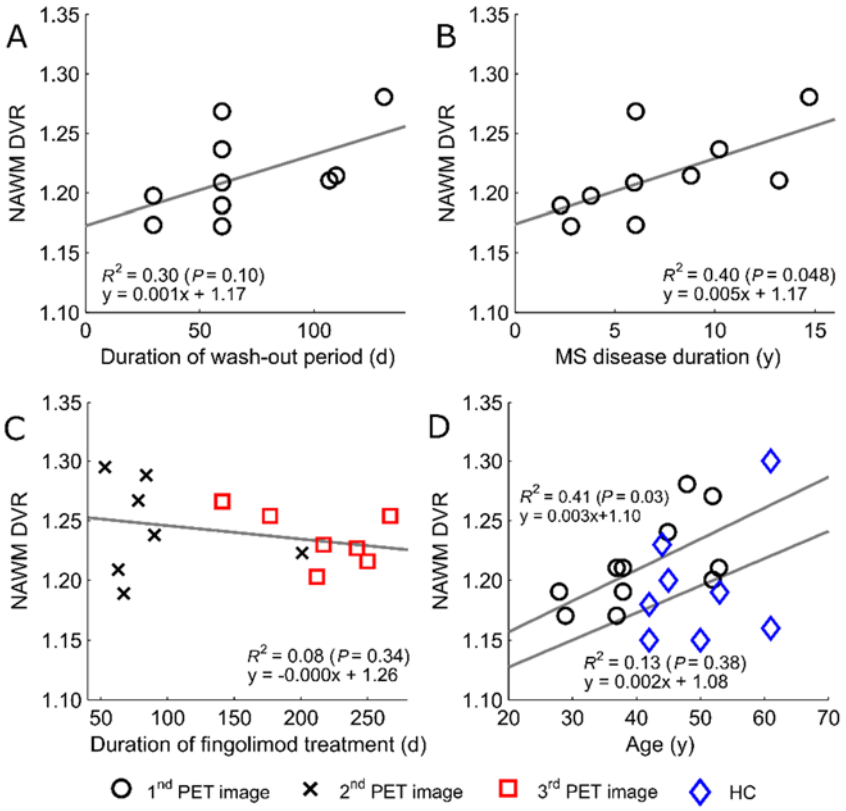

FIGURE 4. Longer washout period, longer disease duration and higher age associate with higher microglial activation in the NAWM. Correlations are shown between (A) duration of treatment-free period before the initiation of fingolimod-treatment, and baseline ^{11}C-(*R*)-PK11195 binding in the NAWM (*n* = 10), (B) disease duration and ^{11}C-(*R*)-PK11195 binding in the NAWM at 1st imaging time point (*n* = 10), (C) duration from the initiation of fingolimod to the 2nd and 3rd imaging time points and ^{11}C-(*R*)-PK11195 binding in NAWM in the respective time points (*n* = 7, pooled *n* = 14) and (D) age and ^{11}C-(*R*)-PK11195 binding in NAWM in HC and relapsing-remitting multiple sclerosis patients at the 1st imaging time point. The linear correlations are visualized as regression lines and squared Pearson coefficients in the images, and the corresponding Spearman correlations are (A) 0.616 (*P* = 0.058), (B) 0.754 (*P* = 0.012), (C) 0.238 (*P* = 0.358) and

(D) 0.636 ($P = 0.048$) for patients and 0.450 ($P = 0.313$) for HC, statistically significant at the level of $P < 0.05$

HC = healthy controls; NAWM = normal appearing white matter

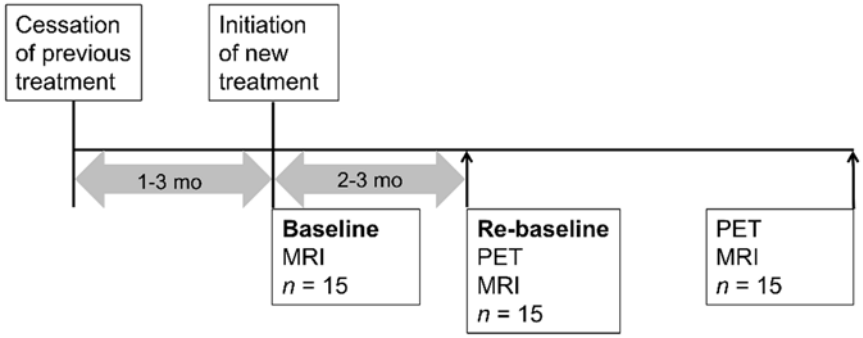

FIGURE 5. A putative design for performing short-term positron emission tomography studies for the evaluation of the efficacy of disease-modifying therapies to reduce the diffuse microglial activation in multiple sclerosis brain. PET = positron emission tomography; MRI = magnetic resonance imaging

Supplemental Table 1. MRI and ^{11}C-(*R*)-PK11195 PET characteristics of the healthy controls (*n* = 8) and RRMS patients (*n* = 10) at baseline and 6 months after treatment.

	Mean (SD) values			Difference of means in RRMS vs. controls	Difference of means in RRMS baseline vs. 6 months
	RRMS		Controls		
	Baseline	6 months	Baseline	% difference *P value*[*]	% change (SD) *P value*[†]
MRI volumes (cm^3)					
Total T2 lesion volume	10.0 (13.1)	11.7 (15.6)	NA	NA	+3.76% (26.0) *0.320*
WM volume	486.4 (53.8)	485.0 (52.4)	485.9 (60.1)	-0.10% *0.333*	-0.27% (0.86) *0.816*
GM volume	420.9 (37.4)	423.9 (39.1)	432.2 (49.1)	+2.61% *0.222*	+0.05% (1.07) *1.000*
NAWM volume	476.4 (60.1)	473.3 (59.9)	NA	NA	-0.66% (0.65) *0.855*
^{11}C-(*R*)-PK11195 DVR					
T2 lesional	1.15 (0.16)	1.04 (0.13)	NA	NA	-12.31% (16.82) *0.040*[‡]
NAWM	1.26 (0.04)	1.27 (0.03)	1.24 (0.03)	-2.00% *0.096*	+0.63% (2.98) *0.512*
GMctx	1.35 (0.06)	1.36 (0.06)	1.32 (0.02)	+2.20% *0.052*[‡]	+0.85% (2.07) *0.223*
Striatum	1.20 (0.05)	1.21 (0.04)	1.17 (0.06)	-2.80% *0.332*	+0.11% (2.31) *0.901*
Thalamus	1.61 (0.15)	1.60 (0.15)	1.47 (0.08)	-9.87% *0.006*[‡]	-0.72% (5.22) *0.737*
Cerebellum	1.13 (0.05)	1.11 (0.04)	1.08 (0.03)	-4.26% *0.072*	-1.21% (2.91) *0.219*
Global (GMWM)	1.24 (0.03)	1.25 (0.03)	1.22 (0.03)	-2.35% *0.021*[‡]	+0.47% (1.89) *0.440*

MRI = magnetic resonance imaging; PET = positron emission tomography; RRMS = relapsing remitting multiple sclerosis; SD = standard deviation; WM = white matter; GM = grey matter; NAWM = normal appearing white matter; DVR = distribution volume ratio; GMctx = gray matter cortex; GMWM = gray matter white matter

[*] Analysis of variance with age as covariate for comparisons between groups

[†] Analysis of variance with Bonferroni correction for comparisons of PET variables within RRMS group

[‡] Statistically significant with the level of $P < 0.05$

Supplemental Table 2. Serial MRI and ^{11}C-(*R*)-PK11195 PET imaging data of RRMS patients (n = 7) at baseline, and 2 months and 6 months after initiation of treatment.

	Mean (SD) values			Differences of means between time points within the RRMS group			
				% change (SD)			
	Baseline	2 months	6 months	baseline vs. 2 months	*P value*[*] 2 vs. 6 months	baseline vs. 6 months	*overall P value*[†]
MRI volumes (cm^3)							
Total T2 lesion volume	4.90 (4.85)	6.33 (7.30)	5.92 (6.79)	+16.8% (11.9)	+15.3% (38.8)	+4.02% (30.6)	
				0.247	*0.334*	*0.302*	*0.541*
WM volume	492.0 (58.5)	491.7 (58.3)	489.8 (57.2)	−0.05% (0.65)	−0.38% (0.57)	−0.43% (0.94)	
				0.865	*0.077*	*0.293*	*0.212*
GM volume	426.6 (31.1)	425.1 (34.5)	426.8 (34.3)	−0.38% (1.49)	+0.40% (1.29)	+0.01% (1.23)	
				0.604	*0.406*	*0.918*	*0.737*
NAWM volume	487.1 (59.5)	485.4 (60.6)	483.9 (59.0)	−0.38% (0.60)	−0.29% (0.48)	−0.66% (0.79)	
				0.512	*0.444*	*0.229*	*0.240*
^{11}C-(*R*)-PK11195 DVR							
T2 lesional	1.16 (0.18)	1.04 (0.20)	1.04 (0.13)	−9.63% (14.33)	+1.00% (9.15)	−9.36% (12.71)	
				0.285	*1.000*	*0.198*	*0.215*
NAWM	1.22 (0.04)	1.24 (0.04)	1.24 (0.02)	+2.12% (4.23)	−0.60% (2.94)	+1.45% (3.50)	
				0.742	*1.000*	*1.000*	*0.540*
GMctx	1.36 (0.07)	1.40 (0.08)	1.38 (0.06)	+3.30% (3.74)	−1.45% (2.24)	+1.74% (1.86)	
				0.192	*0.451*	*0.161*	*0.176*
Striatum	1.22 (0.05)	1.23 (0.03)	1.21 (0.03)	+1.23% (5.00)	−1.38% (3.20)	−0.29% (2.32)	
				1.000	*0.848*	*1.000*	*0.392*
Thalamus	1.58 (0.10)	1.58 (0.07)	1.57 (0.05)	+0.34% (3.59)	−0.81% (3.65)	−0.48% (5.03)	
				1.000	*1.000*	*1.000*	*0.829*
Cerebellum	1.11 (0.05)	1.11 (0.04)	1.10 (0.02)	−0.39% (2.92)	−0.84% (2.75)	−1.26% (3.00)	
				1.000	*1.000*	*0.861*	*0.575*
Global (GMWM)	1.25 (0.04)	1.27 (0.04)	1.26 (0.03)	+2.16% (3.54)	−1.00% (2.20)	+1.07% (2.02)	
				0.491	*0.825*	*0.662*	*0.410*

MRI = magnetic resonance imaging; PET = positron emission tomography; RRMS = relapsing remitting multiple sclerosis; SD = standard deviation; WM = white matter; GM = gray matter; NAWM = normal appearing white matter; DVR = distribution volume ratio; GMctx = gray matter cortex; GMWM = gray matter white matter

[*] Repeated measures analysis of variance used for MRI variables and repeated measures analysis of variance with Bonferroni correction for multiple comparisons of PET variables

[†] Overall *P* value for analysis of variance without correction for multiple comparisons

[‡] Statistically significant with the level of $P < 0.05$

Supplemental Table 3. Demographics of the relapsing-remitting multiple sclerosis patients.

ID	Age (y)	Sex	Disease duration (y)	EDSS baseline	EDSS 6 mo	Relapses during disease	Relapses during study	Washout (mo)
C01	37	F	8.8	3.5	3.5	5	0	3.7
C02	53	F	13.3	3.5	3.5	6	0	3.6
C03	48	F	14.8	2.5	2.5	9	0	4.4
C04	38	F	4.5	2.5	Drop out	3	Drop out	2.0
C05	38	F	6.0	2.5	2.0	2	0	2.0
C06	52	F	3.8	2.5	2.5	4	0	1.0
C07	45	F	10.3	2.0	2.0	4	0	2.0
C08	28	F	2.3	2.0	1.5	3	0	2.0
C09	29	F	2.8	3.0	3.5	8	0	2.0
C10	37	M	6.1	3.0	2.0	2	0	1.0
C11	52	F	6.1	2.5	2.5	4	0	2.0

C = case, F = female, M = male, EDSS = expanded disability status scale